COMMUNICATION

ChemComm
www.rsc.org/chemcomm

Size-controllable luminescent single crystal CaF_2 nanocubes†

Xiaoming Sun and Yadong Li*

Department of Chemistry and the key laboratory of Atomic and Molecular Nanosciences (Ministry of Education), Tsinghua University, Beijing, 100084, P. R. China

Received (in Cambridge, UK) 1st April 2003, Accepted 21st May 2003
First published as an Advance Article on the web 18th June 2003

Single crystal CaF_2 nanocubes were synthesized by a simple hydrothermal method with the absence of surfactants. Rare earth ions were introduced into the fluorite lattice by a chemical modified process.

Inorganic nanoparticles with controllable and uniform size and shape, such as nanospheres, nanorods and nanocubes, have attracted vast attention because of their unique size- and shape-dependent properties and great potential applications.[1–9] Manipulation of the morphology and further functionalization, which are both critical for utilization of these nanoparticles,[10] are great challenges for materialists to overcome. Recently a breakthrough was made in the synthesis of nanocubes. Monodispersed noble metal and Cu_2O nanocubes were prepared by controlled oxidation–reduction reactions in surfactant solutions.[8,9] Here we report the synthesis of single crystal CaF_2 nanocubes through a simple precipitation and hydrothermal procedure in the absence of surfactants. The morphology of the final products could be manipulated through controlling the synthetic parameters such as concentration and pH value. Furthermore, since CaF_2 is used as a host material for rare earth ions[11] these nanocubes could be functionalized by a simple chemical modified method to induce rare earth ions (*e.g.* Eu^{3+} and Tb^{3+}) into the cubes, which endowed the nanocubes with luminescent (*e.g.* red and green) properties and provided new opportunities for diagnosis as a luminescent biological label[12] as well as realizing solid state light emitters and control of chromaticity.

The preparation involved the precipitation of Ca^{2+} and F^- at a low concentration and consequent hydrothermal treatment at 120 °C. In a typical procedure, 2 mmol NaF and 1 mmol $Ca(NO_3)_2$ (A.R., both from Beijing Chemical Reagents Factory) were each dissolved in 20 ml deionized water to form clear solutions. Then the two solutions were mixed under vigorous stirring. The suspension was stirred for 10 min before being transported into a 40 ml Teflon-lined autoclave. After 10–20 hours of hydrothermal treatment at 120 °C, the autoclave was cooled in air naturally. Products were obtained after centrifugation and oven drying.

Trivalent rare earth ions (Eu^{3+} and Tb^{3+}) were introduced into the fluorite lattice by following procedure: 0.04 g CaF_2 nanocubes were redispersed into 4 ml solutions of rare earth ions such as Eu^{3+} and Tb^{3+} with a concentration of 0.05 M. The suspensions were supersonicated for 30 min and aged for 20 hours before centrifugation and oven drying. Following that, the powder was calcined at 450 °C for 3–5 hours in an inert atmosphere.

The phase purity of the as-prepared products was evidenced with a Bruker D8 advance X-ray diffractometer with monochromatized Cu Kα radiation (λ = 1.5418 Å). All the reflections of the XRD pattern in Fig. 1a could be readily indexed to a pure face centered cubic phase [space group: *Fm*3*m* (225)] of CaF_2 with lattice constant a = 5.44 Å, compatible with the literature value of a = 5.4355 Å (JCPDS 772096).

The morphology of the final products was characterized with a Hitachi H-800 transmission electron microscope operated at 200 kV. A typical image of the final products is shown in Fig. 1b.

Most of the final products were square (Fig. 2a) with a mean edge length of 350 ± 30 nm from 200 measured particles. Besides the square products, about 10% of the particles appeared hexagonal (Fig. 2d). The square and hexagonal symmetrical select area electron diffractions (SAED) recorded on corresponding individual square and hexagonal nanoparticles (Fig. 2b & e) could be attributed to [001] and [111] zone axis diffractions of fcc CaF_2, which indicated that each particle was a single crystal. Additionally, it was found that the four corners of the square particles showed relatively slight contrast, which implied the samples might be truncated cubes since the slighter contrast corresponded to thinner parts in the TEM. This was evidenced with a scanning electron microscope equipped with a Strata DB235 Focusing Ion Beam (FIB). The SEM image of an individual square nanocube (Fig. 2c) indicated that the nanocube was heavily truncated and enclosed with crystal faces of {110} and {111} besides the {001} faces.

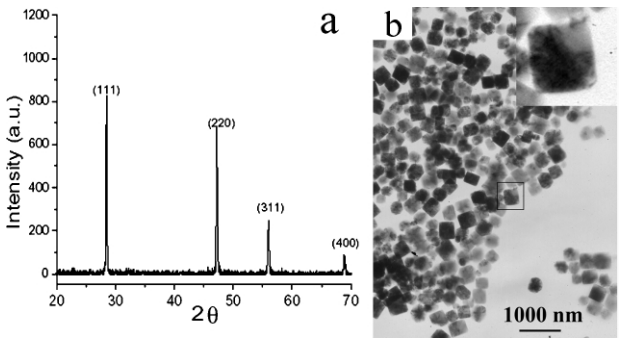

Fig. 1 a) XRD patterns of CaF_2 nanocubes. b) A typical TEM image of CaF2 nanocubes. Inset: a further magnified cube.

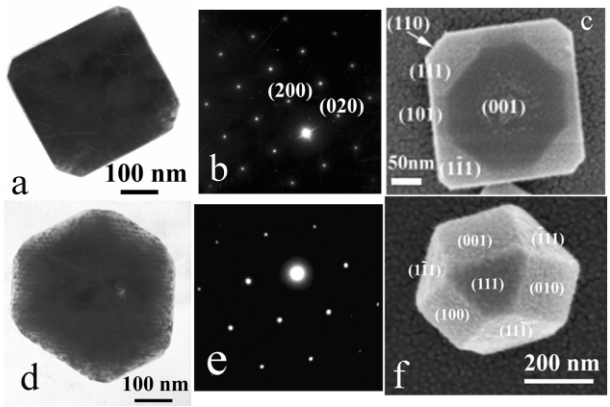

Fig. 2 TEM and SEM images of individual nanocubes: a/d) square/hexagonal particles; b/e) the corresponding ED patterns; c/f) SEM images of individual square/hexagonal particles with enclosing crystal faces labeled.

† Electronic supplementary information (ESI) available: two TEM images and two PL spectra. See http://www.rsc.org/suppdata/cc/b3/b303614f/

DOI: 10.1039/b303614f

The eight heavily truncated corners were consistent with the contrast analysis on the TEM image (Fig. 2a). For the hexagonal particles shown in Fig. 2f, the cubes were so heavily truncated that their {110} crystal faces disappeared because of the encounter of two {111} faces. This kind of nanoparticle was named a "truncated octahedron" in previous work.[13,14] So the different profiles in TEM observation merely resulted from their different supporting crystal faces on the carbon grids used for TEM observation.

Further study suggested that the morphology of the final products strongly depended on the concentration of reactants. A critical concentration was found to be about 0.03 M using $[Ca^{2+}]$ as standard and $[Ca^{2+}] : [F^{-}] = 1 : 2$. When the concentration was below the critical value, the size of particles could be manipulated by changing the amount of reactants. Fig. 3a, b and c show the products corresponding to concentrations of 0.006 M, 0.0125 M, 0.025 M, respectively. Their corresponding size increased from less than 100 nm to 200 nm, and then to about 350 nm, which is almost linear with the concentration. Note that when the size was as small as 100 nm, hexagonal particles were dominant, indicating the truncated octahedra as main products. This was considered to be related to the enhanced effects of surface energy in the smaller particles, which led to more stable {111} faces being exposed.[13,15] However, as the concentration was increased over the critical value, the growth of nanocrystals tended to be irregular, which implied the nucleation and growth behavior were out of the kinetic control (see ESI†).

It was also found that increased acidity favooured narrower size distribution and less truncation. The products obtained at pH = 1 (Fig. 4a) with a concentration of 0.0125 M exhibited almost exclusively square samples enclosed with {001} faces, indicating the cubes were slightly truncated. This might be related to the formation of molecular HF, which affected the formation of CaF_2. Increasing the pH value to 9 led to nanoparticles with coarse surfaces (see ESI†). These results indicated that the *R* value, the growth rate along $<100>$ compared to that along $<111>$, might be manipulated by adjusting the pH value,[14] and finally resulted in nanocubes with different truncation degrees. High-resolution TEM (JEOL-2010F, 200 kV) was used to further investigate the microstructure of the CaF_2 nanocubes (Fig. 4b). The partly magnified image shown in Fig. 4c exhibited satisfactory two-dimensional crystal lattices.

Since CaF_2 is a widely used host material for rare earth ions,[11,16,17] a functionalization approach was undergone on the nanocubes by a solution-based chemical modifying process. Bright red or green luminescence was observed for Eu(III) or Tb(III) doped CaF_2 nanocrystals, respectively. The major peak positioned at 589 nm for Eu doped CaF_2 was attributed to the $^5D_0 \rightarrow {}^7F_1$ transition.[18] The green emission for the Tb doped sample positioned at 546 nm was attributed to $^5D_4$–^7F_J electron transitions of Tb ions.[19] Further study on the full-color simulation and up-conversion emission in the multi-doped cubes is still in progress. These luminescent properties showed that these nanocubes with tunable size distribution and truncation degree can be functionalized with ease, and might find applications in many fields, such as biological labels,[12] visible electroluminescent devices,[16,17] as well as chromaticitic controllable advanced flat-panel display applications.[20]

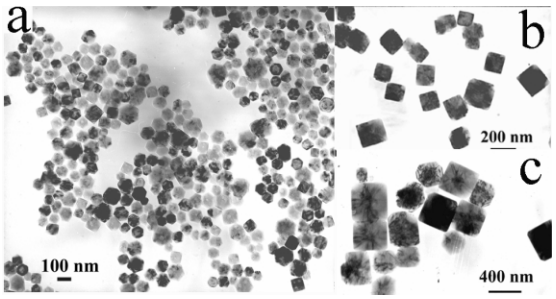

Fig. 3 TEM images of samples prepared with different concentrations: a) 0.006 M; b) 0.0125 M; c) 0.025 M.

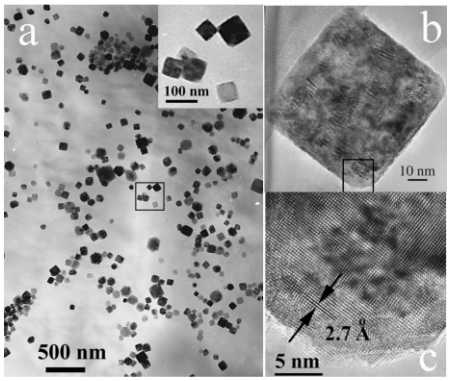

Fig. 4 TEM images of products prepared at pH = 1;. a) a general image (inset, a partly magnified image); b) HRTEM image of an individual CaF_2 nanocube; c) the further magnified image of the circled area in Fig. 4b showing the crystal lattices.

This work was supported by NSFC (20025102, 50028201, 20151001), the Foundation for the Author of National Excellent Doctoral Dissertation of P. R. China, and the state key project of fundamental research for nanomaterials and nanostructures.

Notes and references

1 R. C. Jin, Y. W. Cao, C. A. Mirkin, K. L. Kelly, G. C. Schat and J. G. Zheng, *Science*, 2001, **294**, 1901–1903.
2 V. F. Puntes, K. M. Krishnan and A. P. Alivisatos, *Science*, 2001, **291**, 2115–2117.
3 F. Kim, J. H. Song and P. D. Yang, *J. Am. Chem. Soc.*, 2002, **124**, 14316–14317.
4 A. M. Morales and C. M. Lieber, *Science*, 1998, **279**, 208–211.
5 J. T. Hu, T. W. Odom and C. M. Lieber, *Acc. Chem. Res.*, 1999, **32**, 435–445.
6 M. A. El-Sayed, *Acc. Chem. Res.*, 2001, **34**, 257–264.
7 N. R. Jana, Z. L. Wang, T. K. Sau and T. Pal, *Curr. Sci.*, 2000, **79**, 1367–1370.
8 Y. G. Sun and Y. N. Xia, *Science*, 2002, **298**, 2176–2179.
9 L. F. Gou and C. J. Murphy, *Nano Lett.*, 2003, **3**, 231–234.
10 C. J. Murphy, *Science*, 2002, **298**, 2139–2140.
11 V. V. Sobolev and A. I. Kalugin, *Inorg. Mater.*, 2002, **38**, 1053–1057.
12 W. C. W. Chan and S. M. Nie, *Science*, 1998, **281**, 2016–2018.
13 J. M. Petroski, Z. L. Wang, T. C. Green and M. A. El-Sayed, *J. Phys. Chem. B*, 1998, **102**, 3316–3320.
14 Z. L. Wang, *J. Phys. Chem. B*, 2000, **104**, 1153–1175.
15 N. H. de Leeuw and T. G. Cooper, *J. Mater. Chem.*, 2003, **13**, 93–101.
16 T. Chatterjee, P. J. McCann, X. M. Fang and M. B. Johnson, *J. Vac. Sci. Technol. B*, 1998, **16**, 1463–1466.
17 T. Chatterjee, P. J. McCann, X. M. Fang, J. Remington, M. B. Johnson and C. Michellon, *Appl. Phys. Lett.*, 1997, **71**, 3610–3612.
18 T. Kushida, *J. Lumin.*, 2002, **100**, 73–88.
19 J. C. Pivin, N. V. Gaponenko, I. Molchan, R. Kudrawiec, J. Misiewicz, L. Bryja, G. E. Thompson and P. Skeldon, *J. Alloys Compd.*, 2002, **341**, 272–274.
20 Y. Kuo and K. Suzuki, *MRS Bull.*, 2002, **27**, 859–863.